



## OPEN ACCESS

## EDITED BY

Tali Czarnowicki,  
University of Miami, United States

## REVIEWED BY

Ravi K. Patel,  
University of California, San Francisco,  
United States  
Zhiqiang Song,  
Army Medical University, China

## \*CORRESPONDENCE

Yuanjie Zhu

✉ zhuyj@smmu.edu.cn

Baiping Dong

✉ 15800598427@139.com

Wei Wang

✉ wwang\_fd@fudan.edu.cn

†These authors have contributed  
equally to this work and share  
first authorship

RECEIVED 16 December 2024

ACCEPTED 10 June 2025

PUBLISHED 27 June 2025

## CITATION

Wang L, Wang B, Peng M, Yang X, Huang S,  
Wang R, Du L, Yao R, Wang W, Dong B and  
Zhu Y (2025) Identification and analysis of  
cuproptosis associated molecular clusters  
and immunological profiles in atopic  
dermatitis.

*Front. Immunol.* 16:1545457.

doi: 10.3389/fimmu.2025.1545457

## COPYRIGHT

© 2025 Wang, Wang, Peng, Yang, Huang,  
Wang, Du, Yao, Wang, Dong and Zhu. This is  
an open-access article distributed under the  
terms of the [Creative Commons Attribution  
License \(CC BY\)](#). The use, distribution or  
reproduction in other forums is permitted,  
provided the original author(s) and the  
copyright owner(s) are credited and that the  
original publication in this journal is cited, in  
accordance with accepted academic  
practice. No use, distribution or reproduction  
is permitted which does not comply with  
these terms.

# Identification and analysis of cuproptosis associated molecular clusters and immunological profiles in atopic dermatitis

Liangzhe Wang<sup>1†</sup>, Bo Wang<sup>1†</sup>, Min Peng<sup>2†</sup>, Xiaoyan Yang<sup>1</sup>,  
Sijia Huang<sup>3</sup>, Ruixin Wang<sup>1</sup>, Lin Du<sup>1</sup>, Ruiqian Yao<sup>1</sup>, Wei Wang<sup>4\*</sup>,  
Baiping Dong<sup>1\*</sup> and Yuanjie Zhu<sup>1,3\*</sup>

<sup>1</sup>Department of Dermatology, Naval Medical Center, Naval Medical University, Shanghai, China,

<sup>2</sup>Department of Ultrasound Diagnosis, Naval Medical Center, Naval Medical University,  
Shanghai, China, <sup>3</sup>School of Medicine, Shanghai University, Shanghai, China, <sup>4</sup>Department of  
Research, Naval Medical Center, Naval Medical University, Shanghai, China

**Background:** Atopic dermatitis (AD) is a chronic skin condition marked by  
persistent itching and dryness. The role of cuproptosis, a novel form of  
programmed cell death, in AD is not yet understood.

**Methods:** The GSE107361 dataset was obtained from the Gene Expression  
Omnibus (GEO) database. Cuproptosis-related genes (CRGs) in AD were  
identified and analyzed, and immune landscape analysis was performed using  
ssGSEA. AD was clustered based on CRGs using ConsensusClusterPlus.  
Weighted gene co-expression network analysis (WGCNA) and differential gene  
expression analysis were conducted. Hub genes between AD clusters were  
identified, and both protein-protein interaction (PPI) and drug-gene interaction  
networks were developed.

**Results:** Three CRGs (DLD, MTF1, and GLS) were significantly upregulated in the  
AD group compared to healthy controls. Notably, four core CRGs (LIAS, LIPT1,  
PDHA1, CDKN2A) distinguished early-onset from adult-onset AD, indicating  
more active cuproptosis in early-onset AD. CRGs were linked to immune cell  
infiltration in AD, highlighting differences in immune microenvironments  
between early- and adult-onset AD. Early-onset AD showed high innate  
immunity, while adult-onset AD had a mix of innate and type 1 adaptive  
immunity. CRG expression identified two molecular subtypes with distinct  
immune infiltration: Cluster 2 (high cuproptosis) had predominant innate  
immunity, while Cluster 1 (low cuproptosis) had adaptive immunity.  
Additionally, 102 hub DEGs were identified through WGCNA co-expression  
network analysis, and 10 hub node genes were identified and potential drugs  
were explored for the management of AD.

**Conclusions:** The study provides insights into the roles of cuproptosis-related processes in the pathogenesis and potential treatment of AD. Finding of key hub genes between the 2 distinct immune infiltration subtypes might inform potential therapeutic strategies for AD.

#### KEYWORDS

cuproptosis, atopic dermatitis, differentially expressed genes, immune infiltration, bioinformatics

## 1 Background

Atopic dermatitis (AD) is a chronic and refractory inflammatory skin disease, characterized by dry skin and intense pruritus (1). It ranks among the most common dermatological disorders globally, impacting approximately 20% of the world's population and imposing a substantial societal burden (2). The pathogenesis of AD is intricate and multifactorial, involving complex interactions among genetic predispositions, environmental influences, and immunological mechanisms (3–5). However, the molecular mechanisms of AD are not well understood, hindering its prevention, diagnosis, and treatment. Inflammation, involving various immune cells like macrophages, dendritic cells, mast cells, neutrophils, T cells, and B cells, plays a significant role in AD's development (6, 7). Furthermore, several studies revealed that early- and adult-onset AD exhibit distinct genetic and immune profiles. For example, adult-onset AD is associated with FLG mutations and Th1 skewing, while early-onset AD shows stronger Th2 polarization. This dichotomy underscores the need for age-stratified analyses.

Copper is an intracellular trace metal essential for numerous biological processes. However, an excess of copper can result in cytotoxicity, although the precise mechanism remains to be fully elucidated (8). *Tsvetkov et al.* were the first to report that cuproptosis represents a copper-dependent and distinct form of cell death, separate from other known types of cell death (9). This form of cell death, which is both copper-dependent and reliant on mitochondrial respiration, occurs through the direct binding of

copper to the lipoylated components of the tricarboxylic acid (TCA) cycle. This interaction causes aberrant aggregation of lipoylated proteins and the depletion of iron-sulfur cluster proteins, ultimately resulting in protein toxic stress and the induction of cell death (10, 11).

Recent studies highlight cuproptosis as a key factor in inflammatory disorders. In rheumatoid arthritis, cuproptosis related genes (CRGs) like FDX1 and LIAS increase synovial fibroblast growth and macrophage polarization, worsening joint inflammation (12). In ulcerative colitis, LIPT1 and PDHA1-related cuproptosis disrupts epithelial cells, advancing the disease (13). Notably, in psoriasis, a cutaneous inflammatory disease, cuproptosis causes mitochondrial stress and keratinocyte apoptosis through lipoylation, indicating a common mechanism in immune-related skin conditions (14). However, cuproptosis's role in AD remains unexamined. Considering AD's complex immune environment and mitochondrial dysfunction, we hypothesize that CRGs may orchestrate immune cell infiltration and inflammatory responses in AD, contributing to its clinical heterogeneity between early- and adult-onset subtypes. Understanding cuproptosis and CRGs in AD's immune environment is crucial for exploring its pathogenesis.

The Gene Expression Omnibus (GEO) is a comprehensive database of gene expression datasets related to various diseases (15). These datasets provide crucial information for gaining new insights using different methods. Bioinformatics has become a reliable tool for analyzing existing data (16). In this context, Weighted Gene Co-expression Network Analysis (WGCNA) was used to group selected genes into biological functional modules, which can help explain disease mechanisms (17).

This study utilized the GSE107361 dataset to explore the impact of CRGs on the immune microenvironment in AD, focusing on immune-infiltrating cells, immune-response gene sets, and human leukocyte antigen (HLA) genes. AD samples were categorized into two molecular subtypes, with key molecules identified through the WGCNA co-expression network, highlighting turquoise and yellow modules. A protein-protein interaction network was constructed from 102 hub genes, derived from the intersection of module key genes and 357 differentially expressed genes. Ten hub node genes were identified, suggesting potential therapeutic drugs via DGIdb database interactions. This research may provide new diagnostic biomarkers or therapeutic targets for AD.

**Abbreviations:** AD, Atopic dermatitis; GEO, Gene Expression Omnibus; CRGs, Cuproptosis-related genes; WGCNA, Weighted gene co-expression network analysis; DEGs, Differentially expressed genes; TCA, Tricarboxylic acid; HLA, Human leukocyte antigen; FDX1, Ferridoxin 1; DLD, Dihydrolipoamide dehydrogenase; DLAT, Dihydrolipoamide acetyltransferase; LIAS, Lipoic acid synthetase; GLS, Glutaminase (); LIPT1, Lipoyltransferase 1; MTF1, Metal regulatory transcription factor 1; PCA, Principal component analysis; DGIdb, Drug-Gene Interaction Database; CDF, Cumulative distribution function; PCA, Principal component analysis; AI-subtype, Adaptive-immunity predominant subtype; II-subtype, Innate-immunity predominant subtype; GS, Gene significance; MM, Module membership; cIMiD, Cutaneous immune-mediated inflammatory disease.

## 2 Methods

### 2.1 Data collection and preprocessing

The gene expression microarray data GSE107361 were downloaded from the National Center Biotechnology Information Gene Expression Omnibus (NCBI-GEO) database (<https://www.ncbi.nlm.nih.gov/geo/>, accessed on 15 March 2023). A total of 79 AD patients and 29 adjunct healthy control samples (52 early-onset samples and 56 adult-onset samples) were involved in the present study. During data preprocessing, we retained the samples with both the expression data and the clinical information for analysis, and if there is no probe or multiple genes corresponding to one probe, it is discarded, and if multiple probes correspond to the same gene, the median value is used as the expression amount of the gene. Cuproptosis-related genes were identified from the previous literature (9). A total of 10 genes closely related to cuproptosis were obtained for subsequent analysis, including CDKN2A, FDX1, DLD, DLAT, LIAS, GLS, LIPT1, MTF1, PDHA1, and PDHB.

### 2.2 Chromosome location and protein-protein interaction network of CRGs

Genomic locations of the 10 CRGs in chromosomes were demonstrated using Circos. PPI networks of the CRGs were created from the Search Tool for the Retrieval of Interacting Genes/Proteins (STRING) database, and an interaction score > 0.4 was considered as statistically significant, and hiding individual target protein nodes (18). The data obtained from the String database were input into Cytoscape3.8.0 to visualize the PPI network.

### 2.3 Identification of differentially expressed genes in the CRGs

Based on GSE107361 data, we used Wilcoxon test to analyze the expression of 10 CRGs between AD samples and healthy samples. The DEGs were further identified by the limma package (19) between AD samples and healthy samples. Heat map and box plot were drawn to demonstrate the expressions of DEGs between the two groups. Similarly, the DEGs between AD samples from children and adult patients were identified and illustrated.

### 2.4 Involvement of CRGs in immune regulation of AD

To examine the role of CRGs in the immune regulation of AD, we employed single-sample gene set enrichment analysis (ssGSEA) to quantify immune cell infiltration. Based on GSE107361 data, we conducted a comparative analysis of immune cell infiltration between AD samples and healthy controls and assessed the

Spearman correlation between CRGs and immune-infiltrating cells. Furthermore, we validated these findings using the GSE65832 bulk RNA-seq dataset and GSE269981 scRNA-seq dataset comparing AD samples with healthy controls.

Differences in immune response gene set enrichment scores between AD and normal samples were analyzed, and immune response gene sets were downloaded from the immport database (<https://www.immport.org/shared/genelists>) for a total of 17 immune response gene sets, and spearman correlations between CRGs and immune response gene set enrichment scores were analyzed. Additionally, HLA gene differences between disease and normal samples (PMID: 33724691, 17 HLA genes, see supplementary file HLA) were analyzed, and spearman correlations between cuproptosis-related genes and HLA genes were analyzed. Using the same method as above, the immune infiltration, HLA gene difference and immune response gene set among children vs adults patients were analyzed.

### 2.5 Classification of AD samples into two biologically distinct subtypes based on CRGs

To classify AD samples into distinct subtypes based on the expression level of CRGs. The consensus clustering analysis was conducted using the Consensus Cluster Plus package in R software. Optimal clustering K was used and in order to ensure the stability of classification, 1000 repetitions were performed. Principal component analysis (PCA) was used to show the clustering of different CRG-based subtypes. The differential expressions of CRGs in each clusters were analyzed, and the heat map and box plot of cuproptosis-related genes in each clusters were drawn. The differentially expressed genes (DEGs) between cluster 1 and cluster 2 were analyzed by Limma (with log2 fold change (FC) >1 criteria, adjusted P values < 0.05). The differential expressions between groups were identified by limma, with log2 fold change (FC) ≥ 1 and adjusted P values < 0.05 were considered DEGs. This threshold were selected based on established practices for microarray data to balance sensitivity and specificity.

### 2.6 Functional enrichment analysis and drug-gene interaction network

The GO analysis is a useful method for annotating gene and gene product, and identifying characteristic biological meaning of genome and transcriptome (20, 21). The KEGG is a systematic analysis database of gene function, linking genomic information with high-level functional information (22). Based on CRG clusters, the enrichment scores of GO and KEGG were calculated by ssGSEA algorithm, and the enrichment differences of GO and KEGG between two CRG clusters were analyzed and shown in heat map. PPIs with STRING score > 900 were used to construct the interaction network and visualized by cytoscape (23). The Drug-

Gene Interaction Database (DGIdb) database serves as a central repository for data on drug-gene interactions and druggability gathered from various sources, providing information on drug-gene interactions and druggable genes (24). The drug-gene interaction network was explored by the DGIdb after excluding all non-specific drugs that targeted > 10 genes from the analysis.

## 2.7 Statistical analysis

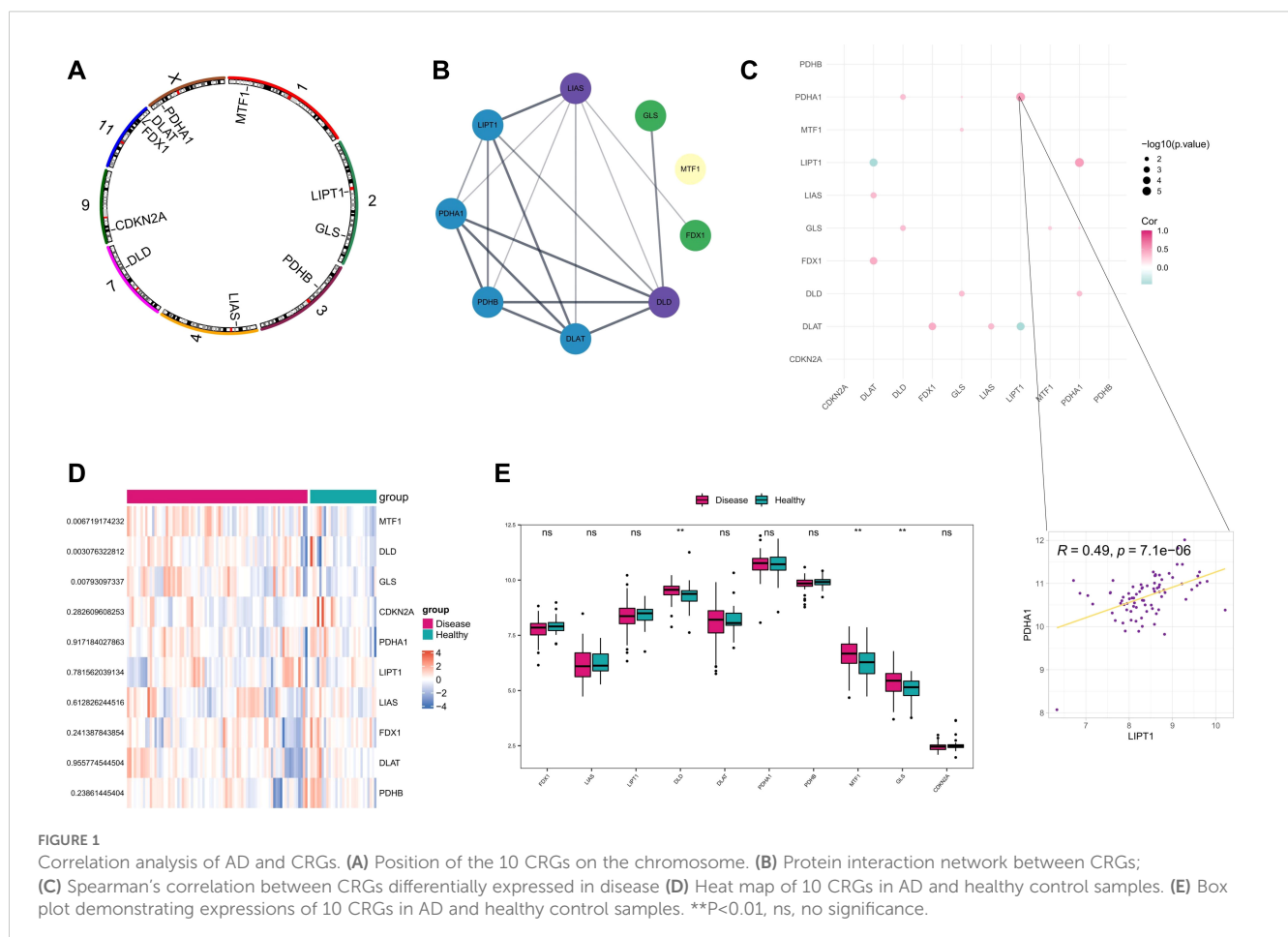
All statistical analyses were conducted in R (version 4.3.0) and SPSS (version 27.0) software. For the comparison of continuous variables between two groups, the Mann-Whitney U test (the Wilcoxon rank-sum test) was used, as the data did not meet the assumptions of normality required for parametric tests. The significance levels of p-values were denoted as follows: NS (not significant,  $p > 0.05$ ), \* ( $0.01 < p \leq 0.05$ ), \*\* ( $0.001 < p \leq 0.01$ ), \*\*\* ( $0.0001 < p \leq 0.001$ ), and \*\*\*\* ( $p \leq 0.0001$ ). Correlation analyses were performed using the Spearman correlation test, which is suitable for non-parametric data. To control for the false discovery rate (FDR) in multiple comparisons, the Benjamini-Hochberg (BH) correction was applied to adjust p-values where appropriate. Adjusted p-values are reported for all analyses involving multiple comparisons.

## 3 Results

### 3.1 Differential expression analysis of CRGs between AD and healthy samples

As indicated previously, 10 genes (FDX1, LIAS, LIPT1, DLD, DLAT, PDHA1, PDHB, MTF1, GLS, and CDKN2A) were demonstrated to be associated with cuproptosis. First, we analyzed the location of the 10 CRGs on the chromosome (Figure 1A), and a PPI network diagram between CRGs was plotted showing the interaction relationship between them (Figure 1B). Analysis of the expression correlations between cuproptosis-related genes revealed that LIPT1 and PDHA1 were most correlated among CRGs in AD samples (Figure 1C). Then, in order to confirm the involvement of these CRGs in AD, we compared the expression patterns of these 10 CRGs between AD and healthy samples downloaded from GEO database (GSE107361 dataset). Consequently, 3 genes (DLD, MTF1, and GLS) were identified as differentially expressed CRGs between AD and healthy samples, and all of them were upregulated in AD samples (Figures 1D, E).

Furthermore, based on the expression data of GSE107361 dataset, we used Wilcoxon to analyze the differential expression of CRGs between the samples from early-onset and adult-onset AD.





The results showed that LIAS, LIPT1, PDHA1, CDKN2A exhibited significantly differential expression between early-onset and adult-onset AD (Figure 2). Among these differentially expressed genes, LIPT1, PDHA1, and CDKN2A were upregulated, while LIAS was downregulated in adult-onset AD samples. These genes are closely related to the condition of immune-infiltrating cells, suggesting the different immune microenvironment between early- and adult-onset AD.

### 3.2 CRGs are involved in the immune regulation of AD

To explore the correlation between the development of AD with immune status, the infiltration of immune cells was analyzed between different samples using ssGSEA. Box plots of the immune cell infiltration scores between AD samples and healthy controls were shown in Figure 3A, and the infiltration scores of activated CD4 T cell, activated CD8 T cell, effector memory CD8 T cell, macrophage, neutrophil, regulatory T cell, type 17 T helper cell and type 2 T helper cell were significantly higher in disease group than that in healthy controls. This suggests a close association between the development of AD and the immune system.

Furthermore, we validated the ssGSEA results using the GSE65832 bulk RNA-seq dataset and GSE269981 scRNA-seq dataset (AD vs. normal controls). The analysis of bulk RNA-seq dataset (Supplementary Figure S1) revealed that the infiltration scores of activated CD4 T cell, effector memory CD8 T cell, neutrophil,

myeloid-derived suppressor cell, and type 17 T helper cell were significantly higher in disease group than that in healthy controls, which was consistent with the ssGSEA results, underscoring the reproducibility of our findings. We annotated the immune cells in the scRNA-seq dataset and compared the frequency of immune cells between AD samples and the healthy samples. As shown in the UMAP plots (Supplementary Figure S2A), the frequency of immune cells (T cells, B cells, neutrophils, NK cells) in the disease samples is significantly elevated than the healthy samples, validating the increased ssGSEA scores. In addition, Bar plots (Supplementary Figure S2B) indicated that AD lesions exhibited higher CD4 T cells, B cells, neutrophils and dendritic cells compared to healthy controls, aligning with ssGSEA results.

The correlation between CRGs and immune cells infiltration were further investigated, and most of CRGs exhibited positive correlation with immune cells. Among them, there was the most significant positive correlation between GLS gene expression and activated CD4 T cell as well as a significant negative correlation between LIPT1 gene expression and neutrophil (Figure 3B). These findings suggest that CRGs may regulate immune infiltration in AD.

Additionally, we compared the difference of immune cells infiltration scores between early-onset and adult-onset AD samples through ssGSEA. As shown in Figure 4, the infiltration scores of activated CD8 T cell, CD56bright natural killer cell, CD56dim natural killer cell, central memory CD4 T cell, effector memory CD8 T cell, macrophage, monocyte, natural killer T cell, neutrophil, regulatory T cell, T follicular helper cell, and type 1 T

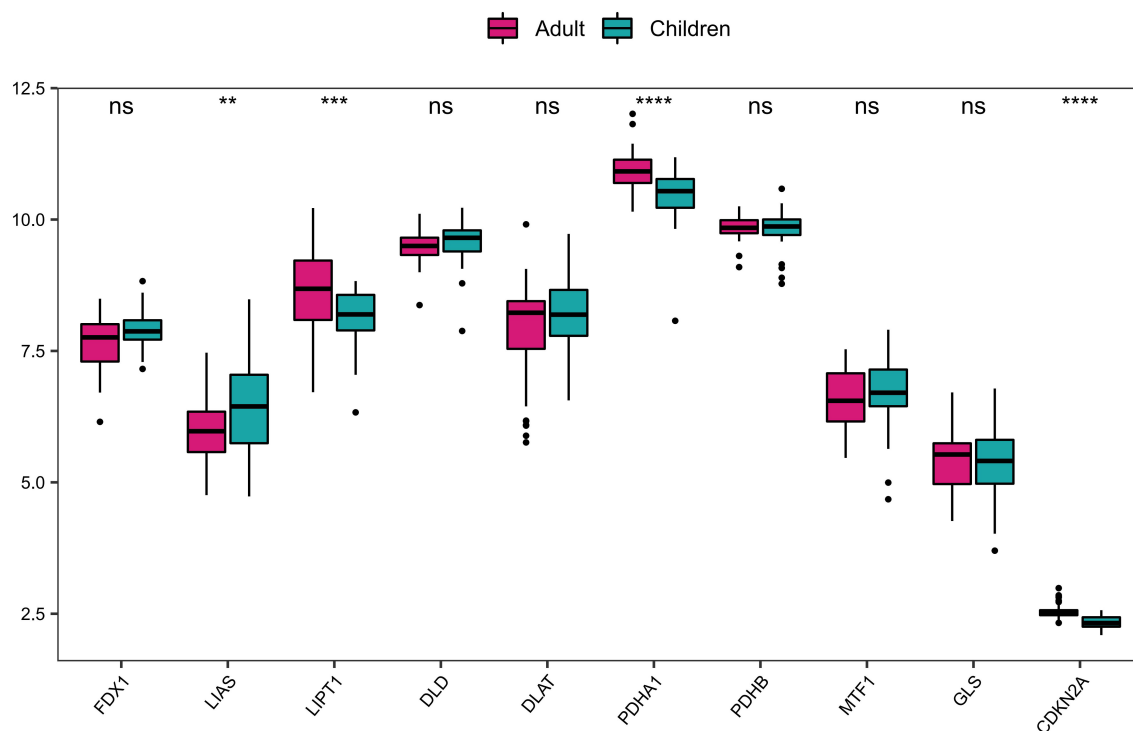
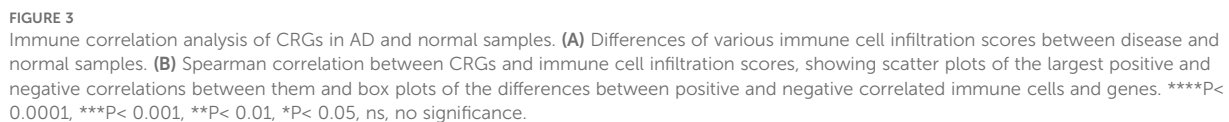
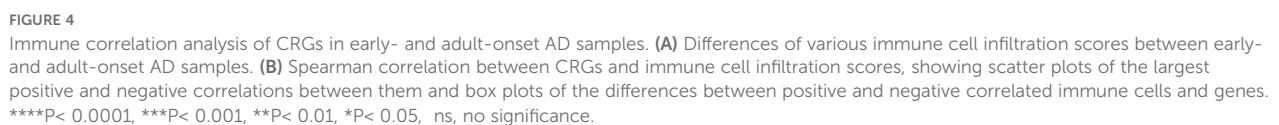


FIGURE 2

The differential expression of CRGs between early-onset and adult-onset AD. \*\*\*\* $P < 0.0001$ , \*\*\* $P < 0.001$ , \*\* $P < 0.01$ , ns, no significance.

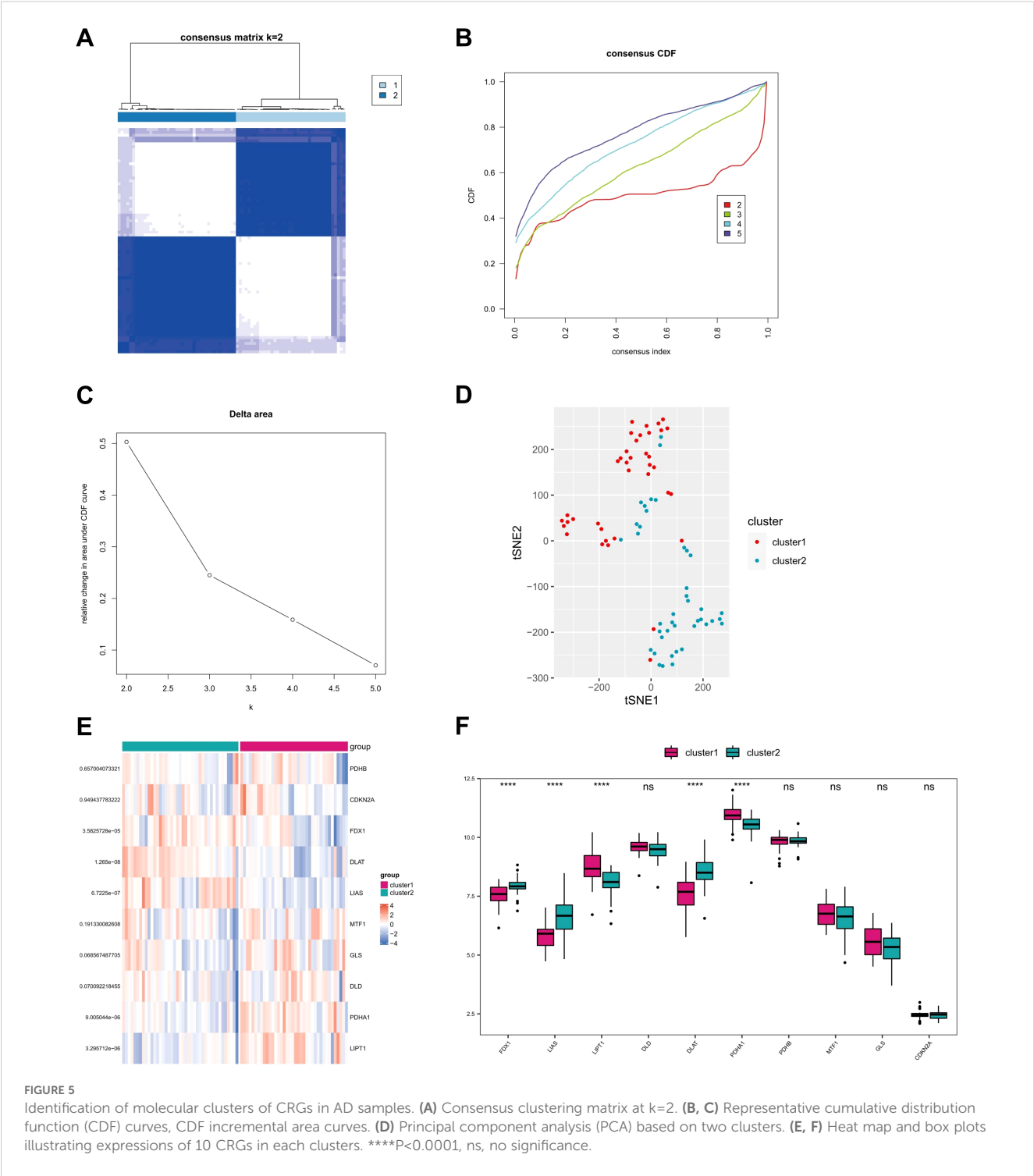


The consensus clustering analysis was performed using the Consensus Cluster Plus package in R software. Based on the expression profile of 10 CRGs in GSE107361 dataset, the optimal clustering stability was chosen when  $k = 2$  (Figure 5A). The curve of CDF values in the range of 0.1-0.9 became nearly smooth when  $k = 2$  (Figures 5B, C). Consequently, the 79 AD patients downloaded from GEO database were divided into two groups. Principal component analysis (PCA) demonstrated a good distinction of the two clusters (Figure 5D). Subsequently, we conducted the differential expression analysis of CRGs between cluster 1 and cluster 2, and three CRGs (FDX1, LIAS, and DLAT) were found



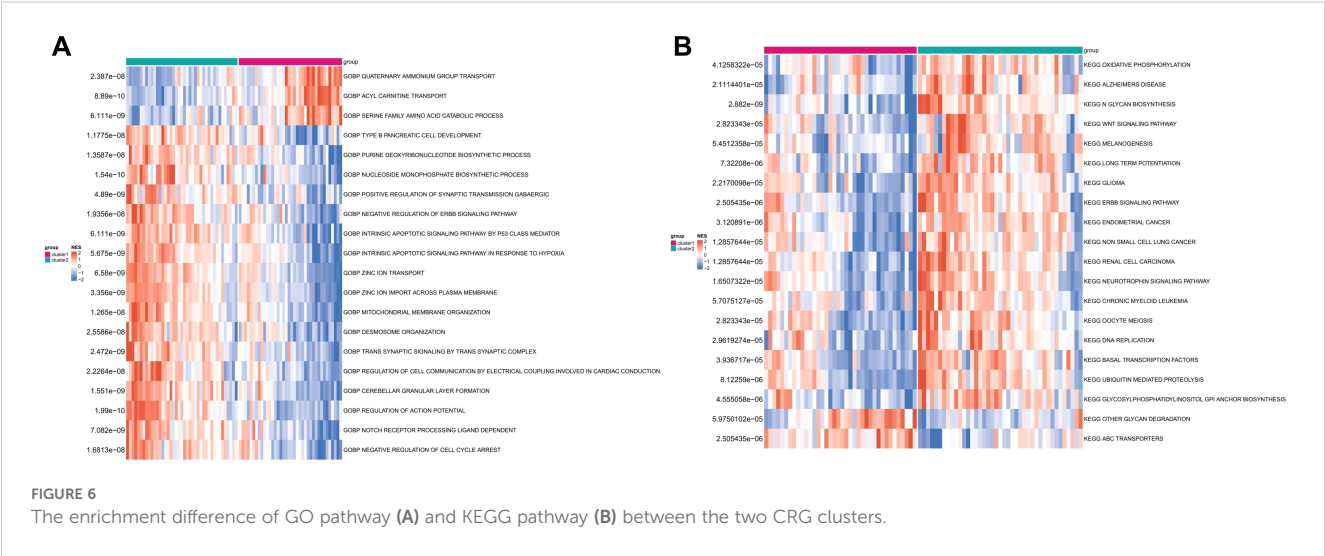
Based on cuproptosis subtype grouping, the enrichment scores of GO and KEGG pathways in different CRG clusters were calculated by ssGSEA algorithm, and the differences of enrichment scores of GO and KEGG pathways between the two clusters were analyzed and shown in heat map (Figures 6A, B). It can be seen that there were significant differences in the enrichment scores of GO and KEGG pathways between the two clusters.

To investigate the differences in immune landscape between the two clusters, the immune infiltrations of cluster 1 and cluster 2 were quantified and analyzed. The results demonstrated that there were significant differences of infiltration scores in activated dendritic cell, CD56dim natural killer cell, effector memory CD8 T cell, gamma delta T cell, immature dendritic cell, mast cell, monocyte, natural killer T cell, and neutrophil between the two clusters. Cluster 1 showed higher levels in CD56dim natural killer cell, effector memory CD8 T cell, and natural killer T cell. We term cluster 1 as adaptive-immunity predominant subtype (AI-subtype), since all of these cells showed a function of cytotoxicity, with more



perforin and granzymes production or a short half-life and little memory potential, which further regulate the adaptive immunity. While cluster 2, termed as innate-immunity predominant subtype (II-subtype), showed higher levels in activated dendritic cell, immature dendritic cell, gamma delta T cell, mast cell, monocyte, and neutrophil (Figure 7A), which were mainly function in innate immunity. The accumulation of immune cells with different functions implies different immune responses, resulting from different stimuli factors. Similarly, there were significant

differences of gene expression in HLA-A, HLA-DMB, HLA-DMA, and HLA-DRA between the two clusters, and cluster 1 showed higher expression in HLA-A, HLA-DMB, HLA-DMA than cluster 2 (Figure 7B). Additionally, the enrichment scores of cytokine receptors, antigen processing and presentation, were significantly different between CRG-based clusters (Figure 7C). Furthermore, we performed the breakdown of early- vs adult-onset samples in clusters 1 and 2. As shown in Table 1, cluster 1 consisted of 68.4% early-onset and 31.6% adult-onset AD samples,



while cluster 2 included 36.6% early-onset and 63.4% adult-onset AD samples. There was a significant correlation between CRGs-based subtype (cluster 1 and cluster 2) and age-based subgroup (adult-onset AD and early-onset AD) ( $P < 0.05$ ), which is consistent with the observation that there were similar immune differences in early- vs. adult-onset comparison and cluster 1 vs. 2 comparison points.

3.5 Identification of key molecules based on co-expression network

Through bioinformatics analysis, a total of 357 differentially expressed genes (DEGs) were found between cluster 1 and cluster 2. To further verify the biological processes related to these DEGs between the two clusters, GO enrichment analysis was performed using the cluster profiler to explore relevant biological process (Figure 8A). Several biological processes, such as epidermis development, muscle system process, skin development, regulation of peptidase activity, keratinocyte differentiation, epidermal cell differentiation, maintenance of location in cell, antimicrobial humoral response, keratinization, neuron cellular homeostasis were enriched.

Based on these gene expression profiling, the weighted co-expression network was constructed using WGCNA. The results showed that co-expression network conforms to the scale-free network, that is, the  $\log(K)$  of the node with  $K$  connectivity is negatively correlated with the  $\log(p(K))$  of the probability of the node occurrence, and the correlation coefficient is greater than 0.8. To ensure that the network was scale-free network, we chose optimal  $\beta = 7$  ( $> 0.85$ , Figure 8B). The next step was to convert the expression matrix to an adjacency matrix, which was then converted to a topological matrix. We used average-linkage hierarchical clustering to cluster genes according to the criteria of mixed dynamic shear trees, and set the minimum number of genes to 30 per gene network module. After identifying gene modules using the dynamic shear method, we calculated the eigengenes of each module once and then performed cluster analysis on the

modules, merging the closer modules into the new module with a set height = 0.25, a total of 23 modules were obtained (Figure 8C).

Pearson correlation coefficients were calculated for the ME of each module and the phenotypic characteristics of the sample, with higher values representing the module being more important. The rows in Figure 8D represent the feature vector genes for each module, and the columns represent the sample phenotypic characteristics, and the correlation coefficients decrease from high to low in descending order from red to blue. The numbers in each box represent the coefficient of correlation between the gene module and the phenotypic characteristics of the sample, and the numbers in parentheses indicate the significance of the P value. Turquoise and yellow were chosen as the key modules. According to the criterion that is module membership ( $MM > 0.6$  and gene significance ( $GS > 0.5$ ), a total of 385 module hub genes (Figures 8E, F) were obtained. Finally, a total of 102 hub DEGs were obtained by crossing the 385 hub genes with the 357 DEGs between CRG-based clusters (Figure 8G).

3.6 Potential therapeutic strategies

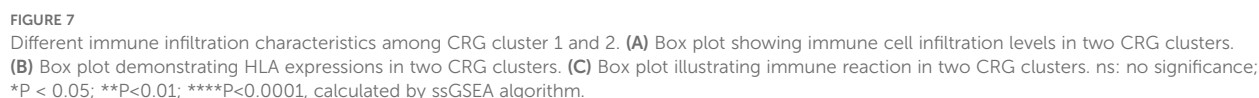
PPI network was constructed based on the above identified hub DEGs (based on STRING database) (Figure 9A). Hub nodes in PPI network were investigated using MCC method of Cytoscape, and 10 genes were obtained as the key hub genes, including YWHAE, CALM1, MYC, RBM15, RUVBL1, YWHAZ, ALYREF, BECN1, GRB1, IQGAP1 (Figure 9B). Further, the interactions between these key genes with

TABLE 1 Breakdown of early- vs adult-onset samples in clusters 1 and 2.

Age-based subgroup	CRGs-based subtype	
	Cluster 1 (38)	Cluster 2 (41)
Adult-Onset	26 (68.4%)	15 (36.6%)
Early-Onset	12 (31.6%)	26 (63.4%)

Statistical Test: Significant association between clusters and age groups ( $\chi^2 = 6.7822$ ,  $P < 0.05$ ).





## 4 Discussion

Atopic dermatitis is a refractory inflammatory skin disease manifested as dry skin, intense itching, and intense itch, bringing increasing medical burden worldwide in the past few decades (25). It has multiple risk factors involved in the interaction between genetic

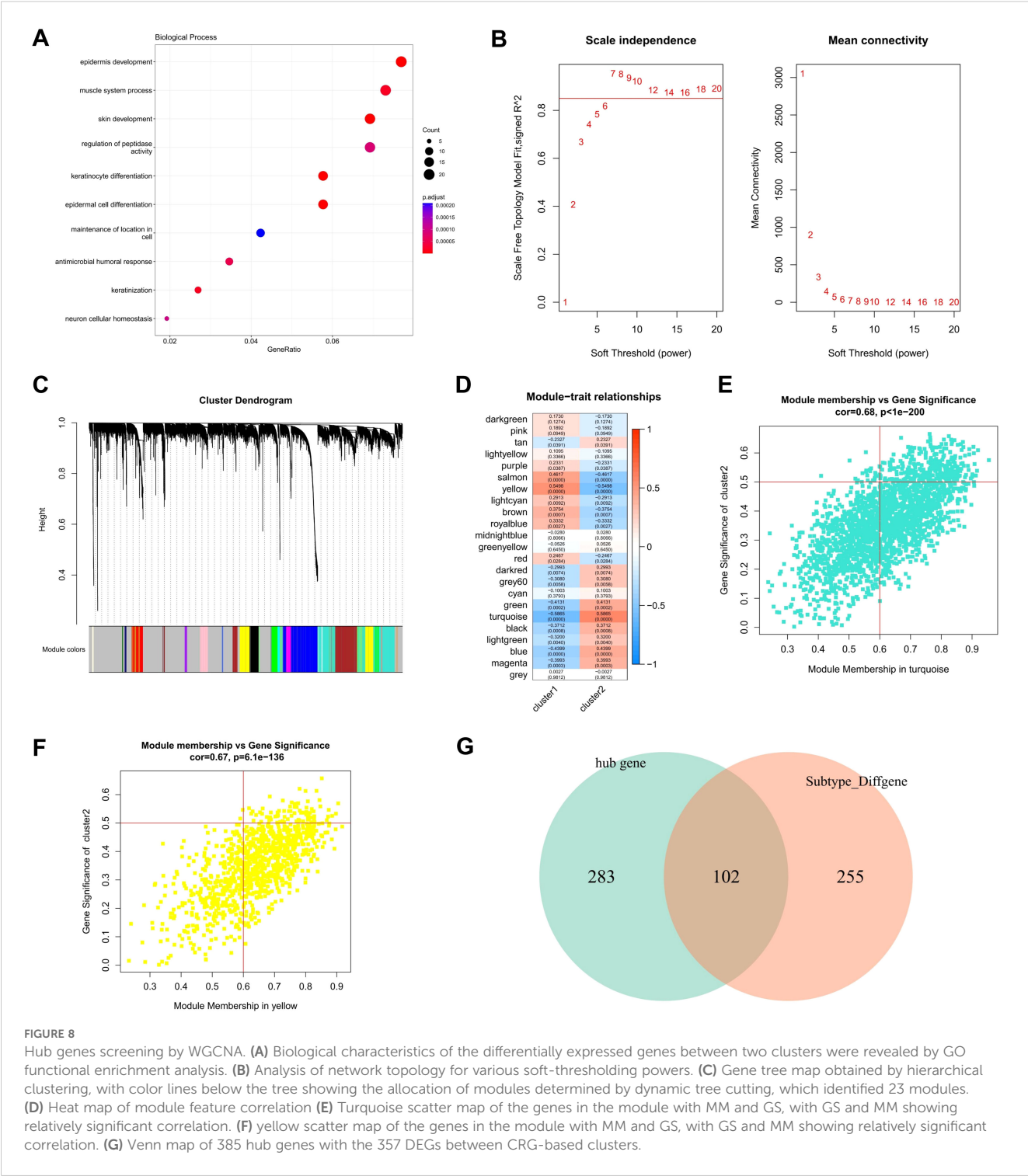
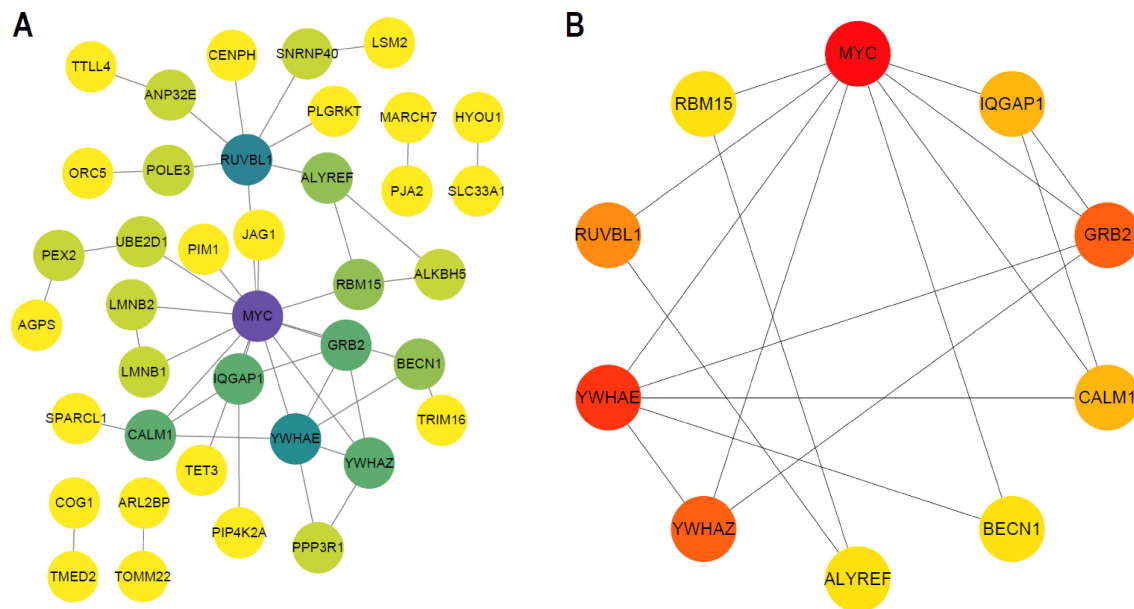


**FIGURE 8** Hub genes screening by WGCNA. **(A)** Biological characteristics of the differentially expressed genes between two clusters were revealed by GO functional enrichment analysis. **(B)** Analysis of network topology for various soft-thresholded powers. **(C)** Gene tree map obtained by hierarchical clustering, with color lines below the tree showing the allocation of modules determined by dynamic tree cutting, which identified 23 modules. **(D)** Heat map of module feature correlation **(E)** Turquoise scatter map of the genes in the module with MM and GS, with GS and MM showing relatively significant correlation. **(F)** Yellow scatter map of the genes in the module with MM and GS, with GS and MM showing relatively significant correlation. **(G)** Venn map of 385 hub genes with the 357 DEGs between CRG-based clusters.

susceptibility and various environmental stimuli (26, 27). Due to the unclear etiopathogenesis and complex pathophysiological process of AD, its prevention and treatment remain challengeable. Therefore, a comprehensive understanding of the genetic backgrounds and cutaneous immune microenvironment is essential for the prevention, treatment, and prognosis evaluation of AD.

Cuproptosis is a newly reported cell death form dependent on mitochondrial respiration and TCA cycle (11). It has been widely studied in various tumor and inflammatory disorders since its

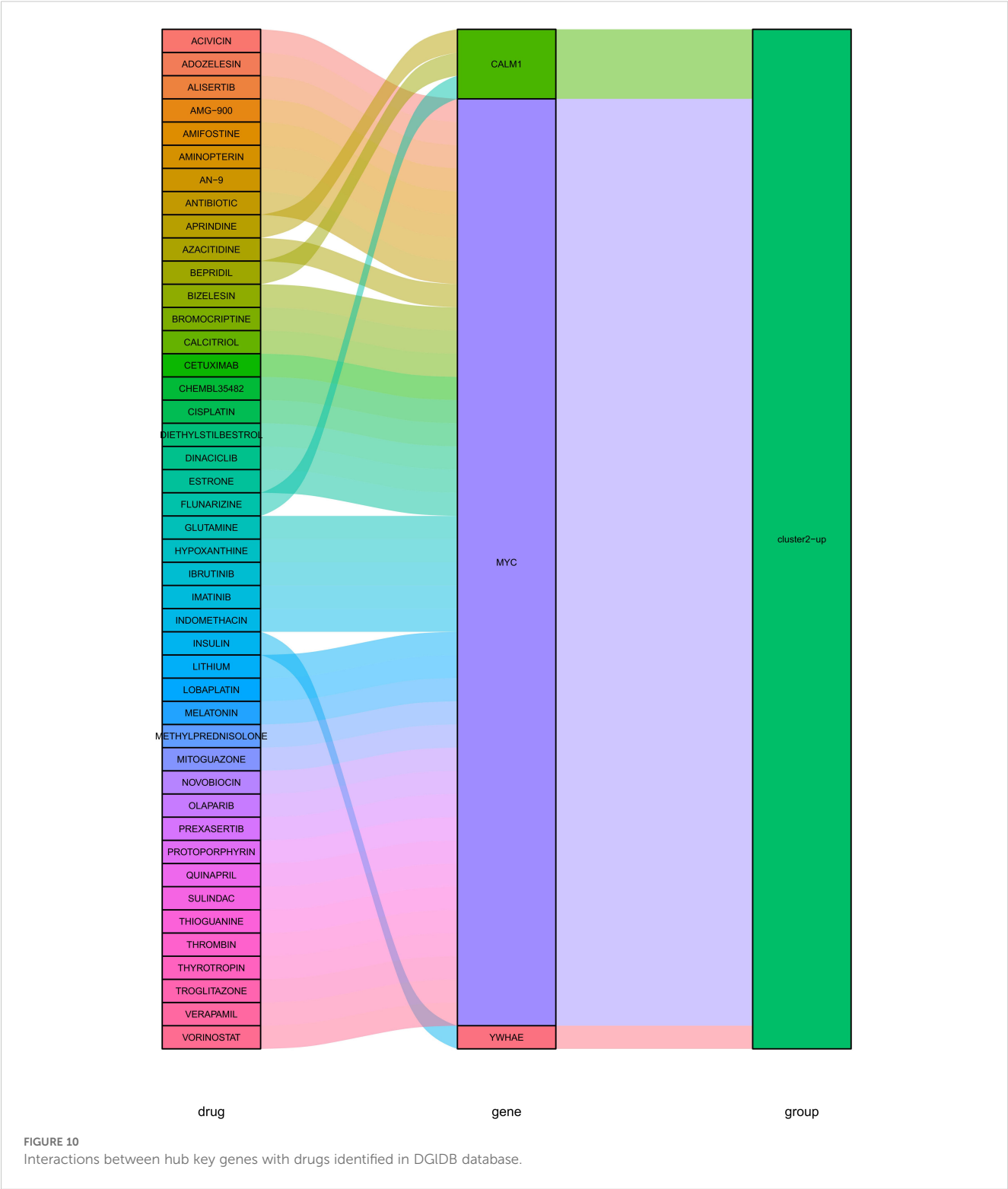
mechanism first being clarified by Tsvetkov et al. in 2022. Recently, several studies have confirmed that cuproptosis-related genes (CRGs) exhibit critical regulatory effects on the immune microenvironment of a variety of inflammatory disorders, such as rheumatoid arthritis, Crohn's disease, and ulcerative colitis (12, 13, 28, 29). In psoriasis, as a cutaneous immune-mediated inflammatory disease (cIMID), cuproptosis has been confirmed being associated with mitochondrial metabolism and facilitated through protein lipoylation (14). However, in AD, another well-



study conducted on ulcerative colitis (UC) revealed that both LIPT1 and PDHA1 are key genes to promote cuproptosis, which can induce the abnormal death of intestinal epithelial cells and lead to the occurrence of UC (28). According to the results in our study, both LIPT1 and PDHA1 were significantly upregulated in adult-onset AD samples. Thus, we deduce that the adult-onset AD patients may have increased risk of UC compared to early-onset AD patients. This speculation was confirmed by a study conducted on the risk of inflammatory bowel disease that adult-onset AD had a 32% increased risk of UC, while early-onset AD did not have increased risk of UC (34). These evidence demonstrate that LIPT1 and PDHA1 may act as the shared targets for the diagnosis, prognosis and treatment of AD and UC.

Several studies have demonstrated that AD is a common disease that is associated with atopic and nonatopic comorbidities, such as asthma, rhinitis, and food allergy, psychiatric, autoimmune, cardiovascular diseases, and certain cancers (35–38). Considering the critical roles of cuproptosis in these diseases (10, 37, 39, 40), CRGs may provide a novel perspective on the underlying mechanisms of AD comorbidity with these diseases.

Notably, LIAS, also a key gene that promotes cuproptosis, was significantly upregulated in early-onset AD samples. LIAS encoded components of the lipoic acid pathway and synthesized a potent antioxidant termed  $\alpha$ -Lipoic acid (LA) in mitochondria and it was found to be associated with oxidative stress and inflammation. Previous studies demonstrated that LIAS expression was highly correlated with the infiltration of immune cells, such as Treg cells, Th1 cells, Th2 cells, NK cells, CD4 T cells, CD8 T cells, neutrophil, macrophages, and et al. (41). The result that LIAS was the only CRGs upregulated in early-onset AD sample suggests the different immune-related characteristics between early-onset and adult-onset AD group. This helps us to recognize the different pathogenesis of



adult-onset and early-onset AD and to conduct different treatment strategies.

What’s more, the immune landscape, including immune cell infiltration, immune response and HLA genes, in AD samples was analyzed using ssGSEA. Most of CRGs exhibited positive correlation with enhanced infiltration and activation of immune cells and immune-related signaling. Among them, there was a significant positive correlation between GLS gene expression and activated CD4 T cell as well as a significant negative correlation between LIPT1 gene expression and neutrophil. CD4+ T cells are known as the principal drivers of AD, and neutrophils can produce reactive oxygen species and led to skin barrier damage in AD.

The concept of precision medicine has promoted the clustering of individual subjects (42). In this study, we performed an

unsupervised clustering analysis based on CRG expression levels and identified two biological clusters in AD samples. The expressions of CRGs exhibited significant difference between the two clusters. Three differentially expressed CRGs, namely FDX1, LIAS, and DLAT, were expressed at significantly higher levels in cluster 2 than cluster 1 and had higher levels of immune infiltration in activated dendritic cell, gamma delta T cell, immature dendritic cell, mast cell, monocyte, and neutrophil. Similarly, there were significant differences of gene expression in HLA-A, HLA-DMB, HLA-DMA, and HLA-DRA between the two clusters, and cluster 1 showed higher expression in HLA-A, HLA-DMB, and HLA-DMA than cluster 2. Pathway enrichment analysis also revealed a number of immune-related pathways that were significantly activated in cluster 2. Taken together, these findings demonstrated that different cuproptosis activation status exhibit distinct immune infiltration characteristics (innate-immunity predominant or adaptive-immunity predominant). Hence, CRGs may regulate the pathological process of AD by mediating these classical pathways associated with cell death, metabolism, and immune response. Future work should also investigate transcriptional regulators (e.g., NF- $\kappa$ B, HIF-1 $\alpha$ ) and epigenetic modifiers (e.g., DNA methylation, histone acetylation) that govern CRG expression in AD. Single-cell ATAC-seq or ChIP-seq in CRG-defined subtypes could elucidate regulatory networks linking copper metabolism to immune dysfunction.

We further performed the breakdown of early- versus adult-onset samples in clusters 1 and 2 and identified a significant correlation between CRG-based subtypes and age-based subgroups. The observed similarities between cluster 1 and adult-onset cases, as well as cluster 2 and early-onset cases, suggest that CRG clusters can be approximately inferred from the age of AD patients, potentially facilitating targeted management strategies for AD. Nonetheless, the presence of early-onset AD patients in cluster 1 and adult-onset, including elderly AD patients, in cluster 2 indicates that classification based solely on clinical age is imprecise. Therefore, classifying AD through CRG analysis may offer more effective guidance for clinical treatment and prognosis.

Furthermore, the 10 hub genes identified (e.g., MYC, CALM1, YWHAE) are mechanistically linked to AD pathogenesis. MYC, a master transcriptional regulator, drives Th17 differentiation and IL-17 production—a cytokine pivotal in AD-associated skin inflammation (43, 44). CALM1 modulates calcium signaling, which is critical for epidermal barrier integrity; its dysregulation may exacerbate transepidermal water loss in AD. YWHAE, a 14-3-3 protein, regulates apoptosis and T cell activation, potentially influencing AD's chronicity (45). Clinically, these genes offer therapeutic potential. For example, Vorinostat—an HDAC inhibitor targeting MYC—suppresses Th17 responses in preclinical models of psoriasis (46, 47), suggesting repurposing potential for AD. Similarly, insulin, which interacts with CALM1, may restore barrier function via calcium homeostasis (48). Future studies should prioritize validating these targets in AD-specific models and clinical trials.

This study is the first to examine the potential roles of cuproptosis and CRGs in AD. Cuproptosis is a unique form of cell death that relies on mitochondrial respiration. Understanding

the role of CRGs in the immune microenvironment of AD could shed light on the disease's development. However, there were still some limitations in our study. First, the predominance of European patients in GSE107361 limits the generalizability of our findings to other ethnic groups. Future studies should validate CRG signatures in diverse cohorts, including Asian and African populations, to account for genetic and environmental heterogeneity. Second, the modest cohort size of GSE107361 (79 AD patients, 29 controls) restricts robust stratification of AD subtypes by clinical severity or comorbidities. Larger, prospectively collected cohorts are needed to validate the prognostic utility of CRG clusters. Third, while bioinformatics approaches robustly identify associations, they cannot establish causality; experimental validation (e.g., CRISPR knockout of DLD or MTF1 in AD models) is essential to confirm mechanistic roles. Lastly, although drug-gene interactions were predicted, their efficacy and safety in AD require rigorous preclinical testing. Addressing these limitations will strengthen the translational relevance of our findings.

## 5 Conclusion

This study is the first to examine CRGs in AD and their impact on the immune microenvironment. It identified three CRGs (DLD, MTF1, GLS) with differential expression between AD and healthy samples, and four CRGs (LIAS, LIPT1, PDHA1, CDKN2A) with significant expression differences between early-onset and adult-onset AD. These genes could be crucial for understanding AD's immunological mechanisms. AD samples were classified into two molecular subtypes based on cuproptosis, corresponding to adaptive or innate immunity predominance. Using WGCNA and gene-drug interaction analysis, 10 hub genes and potential therapeutic drugs, such as acivicin and lithium, were identified for AD management. All these findings suggest that CRGs may play a pivotal role in AD pathogenesis, and ultimately, the identification of CRGs could be a novel perspective on biological markers of diagnosis and treatment of AD.

## Data availability statement

The original contributions presented in the study are included in the article/[Supplementary Material](#). Further inquiries can be directed to the corresponding authors.

## Author contributions

LW: Conceptualization, Writing – original draft. BW: Data curation, Methodology, Writing – original draft. MP: Formal Analysis, Investigation, Methodology, Writing – original draft. XY: Investigation, Methodology, Writing – review & editing. SH: Methodology, Software, Writing – review & editing. RW: Methodology, Software, Writing – review & editing. LD: Investigation, Methodology, Writing – original draft. RY:



Methodology, Writing – review & editing. WW: Conceptualization, Funding acquisition, Project administration, Writing – review & editing. BD: Formal Analysis, Supervision, Validation, Writing – review & editing. YZ: Funding acquisition, Project administration, Supervision, Validation, Writing – review & editing.

## Funding

The author(s) declare that financial support was received for the research and/or publication of this article. This research was funded by the National Natural Science Foundation of China (32201251), and the Shanghai Collaborative Innovation Project (XTCX-KJ-2023-44) and the Basic scientific research project of Naval Medical University (2022MS009).

## Conflict of interest

The authors declare that the research was conducted in the absence of any commercial or financial relationships that could be construed as a potential conflict of interest.

## References

- Bakker D, de Bruin-Weller M, Drylewicz J, van Wijk F, Thijs J. Biomarkers in atopic dermatitis. *J Allergy Clin Immunol.* (2023) 151:1163–8. doi: 10.1016/j.jaci.2023.01.019
- Li H, Zhang Z, Zhang H, Guo Y, Yao Z. Update on the pathogenesis and therapy of atopic dermatitis. *Clin Rev Allergy Immunol.* (2021) 61:324–38. doi: 10.1007/s12016-021-08880-3
- Yang G, Seok JK, Kang HC, Cho YY, Lee HS, Lee JY. Skin barrier abnormalities and immune dysfunction in atopic dermatitis. *Int J Mol Sci.* (2020) 21:134–45. doi: 10.3390/ijms21082867
- Bocheva GS, Slominski RM, Slominski AT. Immunological aspects of skin aging in atopic dermatitis. *Int J Mol Sci.* (2021) 22:32–48. doi: 10.3390/ijms22115729
- Nedoszytko B, Reszka E, Gutowska-Owsiak D, Trzeciak M, Lange M, Jarczak J, et al. Genetic and epigenetic aspects of atopic dermatitis. *Int J Mol Sci.* (2020) 21:24–39. doi: 10.3390/ijms21186484
- Alkon N, Bauer WM, Krausgruber T, Goh I, Griss J, Nguyen V, et al. Single-cell analysis reveals innate lymphoid cell lineage infidelity in atopic dermatitis. *J Allergy Clin Immunol.* (2022) 149:624–39. doi: 10.1016/j.jaci.2021.07.025
- Brunner PM, Leung DYM, Guttman-Yassky E. Immunologic, microbial, and epithelial interactions in atopic dermatitis. *Ann Allergy Asthma Immunol.* (2018) 120:34–41. doi: 10.1016/j.anai.2017.09.055
- Festa RA, Thiele DJ. Copper: an essential metal in biology. *Curr Biol.* (2011) 21:R877–83. doi: 10.1016/j.cub.2011.09.040
- Tsvetkov P, Coy S, Petrova B, Dreishpoon M, Verma A, Abdusamad M, et al. Copper induces cell death by targeting lipoylated tca cycle proteins. *Science.* (2022) 375:1254–61. doi: 10.1126/science.abf0529
- Xie J, Yang Y, Gao Y, He J. Cuproptosis: mechanisms and links with cancers. *Mol Cancer.* (2023) 22:46. doi: 10.1186/s12943-023-01732-y
- Wang Y, Zhang L, Zhou F. Cuproptosis: A new form of programmed cell death. *Cell Mol Immunol.* (2022) 19:867–8. doi: 10.1038/s41423-022-00866-1
- Zhou Y, Li X, Ng L, Zhao Q, Guo W, Hu J, et al. Identification of copper death-associated molecular clusters and immunological profiles in rheumatoid arthritis. *Front Immunol.* (2023) 14:1103509. doi: 10.3389/fimmu.2023.1103509
- Pu Y, Meng X, Zou Z. Identification and immunological characterization of cuproptosis-related molecular clusters in ulcerative colitis. *BMC Gastroenterol.* (2023) 23:221. doi: 10.1186/s12876-024-03236-5
- Lin Q, Zhu J, Chen J, Jia S, Nie S. Significance of cuproptosis-related genes in the diagnosis and classification of psoriasis. *Front Mol Biosci.* (2023) 10:1115091. doi: 10.3389/fmolb.2023.1115091
- Clough E, Barrett T. The gene expression omnibus database. *Methods Mol Biol.* (2016) 1418:93–110. doi: 10.1007/978-1-4939-3578-9\_5
- Uesaka K, Oka H, Kato R, Kanie K, Kojima T, Tsugawa H, et al. Bioinformatics in bioscience and bioengineering: recent advances, applications, and perspectives. *J Biosci Bioeng.* (2022) 134:363–73. doi: 10.1016/j.jbiosc.2022.08.004
- Langfelder P, Horvath S. Wgcna: an R package for weighted correlation network analysis. *BMC Bioinf.* (2008) 9:559. doi: 10.1186/1471-2105-9-559
- Szklarczyk D, Gable AL, Lyon D, Junge A, Wyder S, Huerta-Cepas J, et al. String V11: protein-protein association networks with increased coverage, supporting functional discovery in genome-wide experimental datasets. *Nucleic Acids Res.* (2019) 47:D607–d13. doi: 10.1093/nar/gky1131
- Ritchie ME, Phipson B, Wu D, Hu Y, Law CW, Shi W, et al. Limma powers differential expression analyses for RNA-seq and microarray studies. *Nucleic Acids Res.* (2015) 43:e47. doi: 10.1093/nar/gkv007
- Gene Ontology Consortium. The gene ontology project in 2008. *Nucleic Acids Res.* (2008) 36:D440–4. doi: 10.1093/nar/gkm883
- Ashburner M, Ball CA, Blake JA, Botstein D, Butler H, Cherry JM, et al. Gene ontology: tool for the unification of biology. *Gene Ontology Consortium Nat Genet.* (2000) 25:25–9. doi: 10.1038/75556
- Ogata H, Goto S, Sato K, Fujibuchi W, Bono H, Kanehisa M. KEGG: kyoto encyclopedia of genes and genomes. *Nucleic Acids Res.* (1999) 27:29–34. doi: 10.1093/nar/27.1.29
- Shannon P, Markiel A, Ozier O, Baliga NS, Wang JT, Ramage D, et al. Cytoscape: A software environment for integrated models of biomolecular interaction networks. *Genome Res.* (2003) 13:2498–504. doi: 10.1101/gr.1239303
- Griffith M, Griffith OL, Coffman AC, Weible JV, McMichael JF, Spies NC, et al. Dgidb: mining the druggable genome. *Nat Methods.* (2013) 10:1209–10. doi: 10.1038/nmeth.2689
- Schuler CFT, Billi AC, Maverakis E, Tsoi LC, Gudjonsson JE. Novel insights into atopic dermatitis. *J Allergy Clin Immunol.* (2023) 151:1145–54. doi: 10.1016/j.jaci.2022.10.023
- Weidinger S, Beck LA, Bieber T, Kabashima K, Irvine AD. Atopic dermatitis. *Nat Rev Dis Primers.* (2018) 4:1. doi: 10.1038/s41572-018-0001-z
- Paller AS, Kong HH, Seed P, Naik S, Schar Schmidt TC, Gallo RL, et al. The microbiome in patients with atopic dermatitis. *J Allergy Clin Immunol.* (2019) 143:26–35. doi: 10.1016/j.jaci.2018.11.015
- Sun S, Lv B. Commentary: identification of cuproptosis hub genes contributing to the immune microenvironment in ulcerative colitis using bioinformatic analysis and

## Generative AI statement

The author(s) declare that no Generative AI was used in the creation of this manuscript.

## Publisher's note

All claims expressed in this article are solely those of the authors and do not necessarily represent those of their affiliated organizations, or those of the publisher, the editors and the reviewers. Any product that may be evaluated in this article, or claim that may be made by its manufacturer, is not guaranteed or endorsed by the publisher.

## Supplementary material

The Supplementary Material for this article can be found online at: <https://www.frontiersin.org/articles/10.3389/fimmu.2025.1545457/full#supplementary-material>

experimental verification. *Front Immunol.* (2023) 14:1224127. doi: 10.3389/fimmu.2023.1224127

29. Yuan Y, Fu M, Li N, Ye M. Identification of immune infiltration and cuproptosis-related subgroups in crohn's disease. *Front Immunol.* (2022) 13:1074271. doi: 10.3389/fimmu.2022.1074271

30. Yang C, Wang W, Li S, Qiao Z, Ma X, Yang M, et al. Identification of cuproptosis hub genes contributing to the immune microenvironment in ulcerative colitis using bioinformatic analysis and experimental verification. *Front Immunol.* (2023) 14:1113385. doi: 10.3389/fimmu.2023.1113385

31. Brunner PM, Guttman-Yassky E, Leung DY. The immunology of atopic dermatitis and its reversibility with broad-spectrum and targeted therapies. *J Allergy Clin Immunol.* (2017) 139:S65–s76. doi: 10.1016/j.jaci.2017.01.011

32. Dainichi T, Kitoh A, Otsuka A, Nakajima S, Nomura T, Kaplan DH, et al. The epithelial immune microenvironment (Eime) in atopic dermatitis and psoriasis. *Nat Immunol.* (2018) 19:1286–98. doi: 10.1038/s41590-018-0256-2

33. Johnson MO, Wolf MM, Madden MZ, Andrejeva G, Sugiyama A, Contreras DC, et al. Distinct regulation of th17 and th1 cell differentiation by glutaminase-dependent metabolism. *Cell.* (2018) 175:1780–95.e19. doi: 10.1016/j.cell.2018.10.001

34. Chiesa Fuxench ZC, Wan J, Wang S, Syed MN, Shin DB, Abuabara K, et al. Risk of inflammatory bowel disease in patients with atopic dermatitis. *JAMA Dermatol.* (2023) 159:1085–92. doi: 10.1001/jamadermatol.2023.2875

35. Thyssen JP, Halling AS, Schmid-Grendelmeier P, Guttman-Yassky E, Silverberg JL. Comorbidities of atopic dermatitis-what does the evidence say? *J Allergy Clin Immunol.* (2023) 151:1155–62. doi: 10.1016/j.jaci.2022.12.002

36. Silverberg JL. Comorbidities and the impact of atopic dermatitis. *Ann Allergy Asthma Immunol.* (2019) 123:144–51. doi: 10.1016/j.anai.2019.04.020

37. Liu L, Liang L, Yang C, Chen Y. Machine learning-based solution reveals cuproptosis features in inflammatory bowel disease. *Front Immunol.* (2023) 14:1136991. doi: 10.3389/fimmu.2023.1136991

38. Zhao J, Guo S, Schrod SJ, He D. Cuproptosis and cuproptosis-related genes in rheumatoid arthritis: implication, prospects, and perspectives. *Front Immunol.* (2022) 13:930278. doi: 10.3389/fimmu.2022.930278

39. Chen X, Cai Q, Liang R, Zhang D, Liu X, Zhang M, et al. Copper homeostasis and copper-induced cell death in the pathogenesis of cardiovascular disease and therapeutic strategies. *Cell Death Dis.* (2023) 14:105. doi: 10.1038/s41419-023-05639-w

40. Wang D, Tian Z, Zhang P, Zhen L, Meng Q, Sun B, et al. The molecular mechanisms of cuproptosis and its relevance to cardiovascular disease. *BioMed Pharmacother.* (2023) 163:114830. doi: 10.1016/j.biopha.2023.114830

41. Li Y, Xu B, Zhang J, Liu X, Ganesan K, Shi G. Exploring the role of lias-related cuproptosis in systemic lupus erythematosus. *Lupus.* (2023) 32:1598–609. doi: 10.1177/09612033231211429

42. Czarnowicki T, He H, Krueger JG, Guttman-Yassky E. Atopic dermatitis endotypes and implications for targeted therapeutics. *J Allergy Clin Immunol.* (2019) 143:1–11. doi: 10.1016/j.jaci.2018.10.032

43. Xu D, Xie R, Xu Z, Zhao Z, Ding M, Chen W, et al. Mtor-myc axis drives acinar-to-dendritic cell transition and the cd4(+) T cell immune response in acute pancreatitis. *Cell Death Dis.* (2020) 11:416. doi: 10.1038/s41419-020-2517-x

44. Rothenberg-Lausell C, Bar J, Dahabreh D, Renert-Yuval Y, Del Duca E, Guttman-Yassky E. Biologic and small-molecule therapy for treating moderate to severe atopic dermatitis: mechanistic considerations. *J Allergy Clin Immunol.* (2024) 154:20–30. doi: 10.1016/j.jaci.2024.04.009

45. Rezaei Tavirani M, Bandarian F, Razi F, Razzaghi Z, Arjmand B, Rostami Nejad M. Assessment of nb-uvb effects on skin of atopic dermatitis patients: A network analysis. *J Lasers Med Sci.* (2024) 15:e27. doi: 10.34172/jlms.2024.27

46. Ge Z, Da Y, Xue Z, Zhang K, Zhuang H, Peng M, et al. Vorinostat, a histone deacetylase inhibitor, suppresses dendritic cell function and ameliorates experimental autoimmune encephalomyelitis. *Exp Neurol.* (2013) 241:56–66. doi: 10.1016/j.expneurol.2012.12.006

47. Samuelov L, Bochner R, Magal L, Malovitski K, Sagiv N, Nussbeck J, et al. Vorinostat, a histone deacetylase inhibitor, as a potential novel treatment for psoriasis. *Exp Dermatol.* (2022) 31:567–76. doi: 10.1111/exd.14502

48. Cardoso AL, Fernandes A, Aguilar-Pimentel JA, de Angelis MH, Guedes JR, Brito MA, et al. Towards frailty biomarkers: candidates from genes and pathways regulated in aging and age-related diseases. *Ageing Res Rev.* (2018) 47:214–77. doi: 10.1016/j.arr.2018.07.004